Available online at www.sciencedirect.com
ScienceDirect
MECHATRONICS
Mechatronics 17 (2007) 325–335

Technical note

Design and hybrid control of the pneumatic force-feedback systems for Arm-Exoskeleton by using on/off valve

Chen Ying, Zhang Jia-fan *, Yang Can-jun, Niu Bin

The State Key Laboratory of Fluid Power Transmission and Control, Zhejiang University, Hangzhou 310027, PR China

Received 26 March 2006; accepted 2 April 2007

Abstract

This article models a pneumatic force-feedback system consisting of the double-acting cylinder and a set of high-speed on–off valves, and its fuzzy controller in order to provide an insight into pneumatic system design and force-feedback control requirements of the Arm-Exoskeleton, which is applied in robot-teleoperation and robotics. In modeling, effects of nonlinear flow through the valves, air compressibility in cylinder chambers, and time delay and attenuation of the pressure input in the connecting tubes are considered. Based on this mathematical model, the hybrid fuzzy control method for the precise force-feedback control is proposed and the fuzzy controllers are realized with the Mega8 MCUs as the units of the distributed control system in the Arm-Exoskeleton. At last a series of experiments validated the models and control method.

Keywords: Pneumatic; Force-feedback system; Mathematical model; High-speed on–off valve; Hybrid fuzzy control; Exoskeleton-arm

1. Introduction

The Arm-Exoskeletons with force-feedback have been widely designed and used in the fields of robot teleoperation, haptic interface to enhance the performance of the human operator, also in the exciting applications in surgery planning, personnel training, and physical rehabilitation. These all need a high-performance force actuator. Over the traditional geared servo-electrical motors, the pneumatic actuators have significant advantages in terms of torque-to-mass ratio and its ability to produce high-static forces without overheat dissipating system, which is an important requirement for robot teleoperation and haptic interfaces [1]. We believe that the pneumatic actuators are the ideal force actuator in our Arm-Exoskeleton, ZJUESA. The ZJUESA Arm-Exoskeleton with 6 DOF is designed for the robot manipulator master/slave control, which is used under water. It requires lightweight, good manipulation character, especially clearance.

However, the position and force control of these actuators in applications that require high-bandwidth are somewhat difficult, because of the compressibility of air and its effect both on the actuators and valves [2]. Besides, the highly nonlinear flow through pneumatic system components, and the pressure dropping and time-delay along the connecting tube also result in the control errors. In this paper, we analyze the dynamic behavior of the pneumatic cylinders and high-speed on–off valves, and then build the simple and precise mathematical model of them. According to the given models, a hybrid fuzzy controller is implemented by sets of Mega8 MCUs as the units of the distributed control system for our pneumatic force-feedback system.

The article is arranged such that we present a technical overview of the ZJUESA Arm-Exoskeleton system in Section 2. Then we describe the mathematical models of the elements in the pneumatic system in Section 3 and fuzzy controller design in Section 4. Consequently, the results of the experiments and their analysis are presented in Section 5, followed by discussions and conclusions.

* Corresponding author. Tel.: +86 571 87953096.
E-mail address: caffeezhang@hotmail.com (Z. Jia-fan).

0957-4158/$ - see front matter © 2007 Elsevier Ltd. All rights reserved.
doi:10.1016/j.mechatronics.2007.04.001

2. Relative works

Presence in the unstructured environment, the master/slave robot teleoperaion plays an important role between the operator and the machine. Since the pioneering work of Goertz [3], a number of similar system and schemes have been proposed. In the teleoperation conditions it is found that the force-feedback can give the operator a fidelity feeling of the manipulating, what increases the performance significantly with all measures and reduces spending time. Also the manipulating accuracy is always improved as opposed to only visual or sound feedback.

Since the force-feedback is introduced into the teleoperation, the type of the force actuator has been a hotspot in research. The force actuators can be categorized into following series: servo-electrical motor, hydraulic actuator, pneumatic actuator including artificial muscle, electrorheological fluid and other new types of actuators [4–8]. Among them, the pneumatic actuators have significant advantages over the electrical-servo motors in terms of torque-to-mass ratio and their ability to produce high-static forces without overheating, and have lightweight and clearance merits relative to the hydraulic actuators. Jeong et al. [5] based on the human joint anatomy and introduced the 3RPS parallel mechanism into the exoskeleton-type master arm with pneumatic actuators at the shoulder and wrist multi-degrees joint. We follow this concept and design an Exoskeleton-Arm, ZJUESA, as shown in Fig. 1, for the Schilling underwater master/slave robot manipulation [14]. Fig. 2 explains the schematic diagram of the entire system. The hexagons represent the six key components of the Schilling Robot master/slave control system with its Exoskeleton-Arm Manipulator. The oranges represent the master manipulator system and the blues are slave robot system. The Internet or Ethernet acts as the bridge between these two sides.

However, most of the pneumatic force and position control problems source from the air compressibility and its effect on both the actuators and valves. Due to these difficulties, early use of pneumatic actuators was limited to simple applications where position only required at the two ends of a stroke. In the last decade, with more accuracy mathematical models for the thermodynamic and flow equations in the charging/discharging processes [2,11],

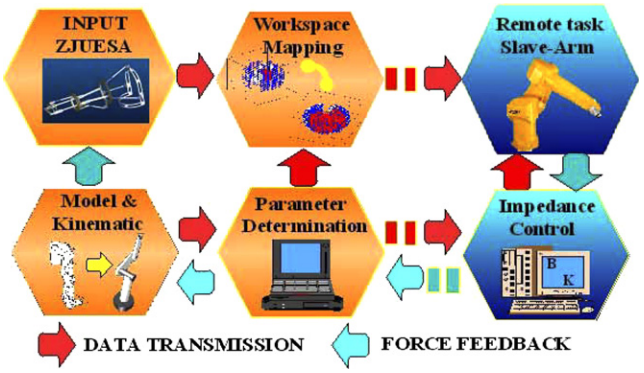

Fig. 2. The schematic diagram of the entire system.

and the intelligent controller developing, nonlinear control techniques were implemented by using digital computers. Bobrow and Jabbari used adaptive control for force actuation and trajectory tracking, applied to an air-powered robot [9]. But the mathematical models used in these controllers assumed no piston seals friction, linear flow through the valve, and neglected the valve dynamics. Ben-Dov and Salcudean developed a force-controlled pneumatic actuator that provided a force with amplitude of 2 N at 16 Hz [10]. Kaitwanidvilai and Parnichkun applied the hybrid adaptive neuro-fuzzy model for the force control, Bang–bang method for the case in which the actual output is far away from the set point, while the hybrid ANFMRC is applied in medium and small error ranges to perform a good response [13]. In addition, the stability of the pneumatic system with the symmetric valve controlled double-acting cylinder is concentrated [20,21]. Unfortunately many of these systems, though successful, use expensive proportional servo valves and pressure sensor feedback loops and the external loads are also assumed to be constant or slowly varying.

In this paper, a hybrid fuzzy controller was designed and the pneumatic force control was implemented, based on the pneumatic cylinder and valve thermodynamic and flow mathematic models with the considering of time delay and attenuation influence along the tube line. Then several experiments were fulfilled and the results were compared with ones obtained by numerical simulation in MATLAB.

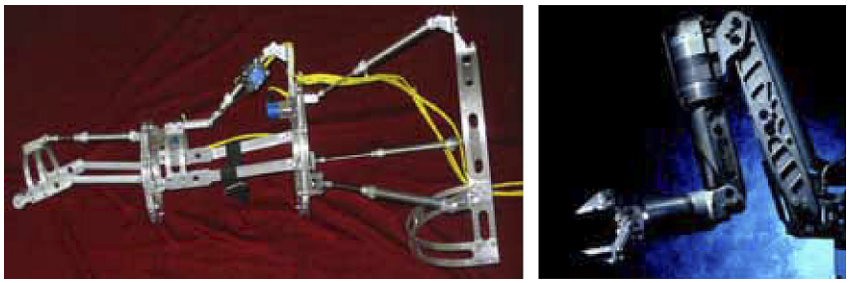

Fig. 1. The Exoskeleton-Arm, ZJUESA, and the schilling slave robot.

3. Model of the force-feedback pneumatic system

A typical pneumatic system consists of force elements (the pneumatic cylinders or motors), commanding devices (valves), connecting tubes, and sensors of position, pressure and force. Fig. 3 shows the scheme of one of the on–off valve-cylinder systems in the ZJUESA. There are total 7 sets of the pneumatic control system, which are independent of each other and work for each actuator respectively.

The high-speed on–off valves, working as the command components in the system, are controlled by the PWM (pulse width modification) signal from the control unit. Rather than the proportional or servo valve, this is an inexpensive and widely used method in the application of position and force control in the pneumatic system [13,16–18] with higher frequency response and simpler control circuit. To simplify the control algorithm, there is just one valve on work in any time. For instance, when a leftward force is wanted, the valve V_1 works and valve V_2 is out of work. We can control the pressure P_1 in the chamber 1 by modifying the PWM signals. The chamber 2 connects to the atmosphere at that time and the pressure P_2 inside the chamber 2 of cylinder is absolute ambient pressure, and vice versa. At each port of the cylinder, there is a pressure sensor to detect the pressure value inside the chamber for the close-loop control. And the throttle valves are equipped for limiting the flow out of the chamber to reduce piston vibrations.

3.1. Cylinder chamber model

As to the charging and discharging process, several models have been put forward. For each model, it is always assumed that:

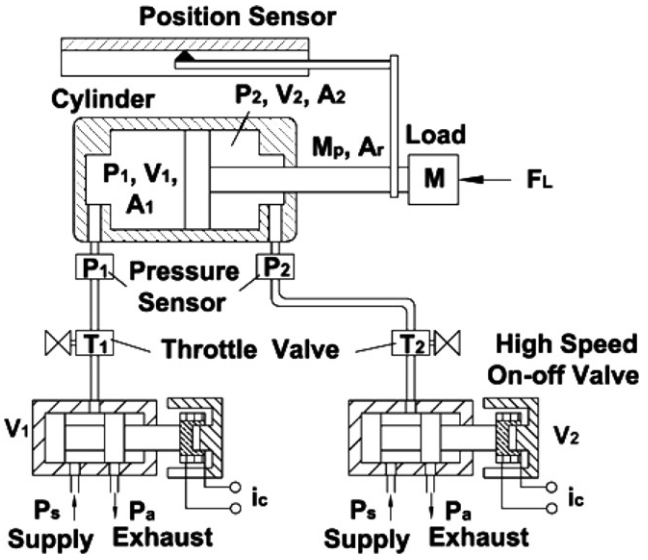

Fig. 3. Schematic representation of the pneumatic cylinder-valve system of the ZJUESA.

- air is the ideal gas;
- the pressure and temperature is homogeneous within the chamber;
- kinetic and potential energy terms are taken out of consideration.

Al-Ibrahim and Otis found experimentally that the temperature inside the chambers lays between the theoretical adiabatic and isothermal curves. The experimental values of the temperature were close to the adiabatic curve only for the charging process. For the discharging of the chamber the isothermal assumption was closer to the measured values [12]. In this article we start from this viewpoint.

In general, the model for a volume of gas contains three basic equations: (1) ideal gas law; (2) the conservation of mass equation or continuity equation; (3) the energy equation.

$$\begin{cases} P = \rho RT, \\ \dot{m} = \frac{\mathrm{d}}{\mathrm{d}t}(PV), \\ q_{\mathrm{in}} - q_{\mathrm{out}} + kC_{\mathrm{v}}(\dot{m}_{\mathrm{in}}T_{\mathrm{in}} - \dot{m}_{\mathrm{out}}T) - \dot{W} = \dot{U}, \end{cases} \tag{1}$$

where, R is the ideal gas constant; $\dot{m}_{\mathrm{in}}$ and $\dot{m}_{\mathrm{out}}$ are the mass flow entering and leaving the chamber; $q_{\mathrm{in}}$and q_{out} are the heat transfer; k is the heat ratio; C_{v} is the heat at constant volume; T_{in} is the temperature of the air entering the chamber and T is atmosphere temperature, here we assume $T_{\mathrm{in}} = T$; $\dot{W}$ is the rate of the change in the work and $\dot{U}$ is the change of internal energy, which can be expressed as following:

$$\dot{U} = \frac{\mathrm{d}}{\mathrm{d}t}(C_{\mathrm{v}}mT). \tag{2}$$

Now substitute $\dot{W} = P\dot{V}$ and $C_{\mathrm{v}} = R/(k-1)$ into Eqs. (1) and (2):

$$q_{\mathrm{in}} - q_{\mathrm{out}} + \frac{k}{k-1}\frac{R}{\rho T}(\dot{m}_{\mathrm{in}}T - \dot{m}_{\mathrm{out}}T) - \frac{k}{k-1}P\dot{V} = \frac{1}{k-1}V\dot{P}. \tag{3}$$

Eq. (3) can be simplified by different heat transfer term. If the charging process is considered as adiabatic, i.e., $q_{\mathrm{in}} - q_{\mathrm{out}} = 0$,

$$\dot{P} = k\frac{RT}{V}(\dot{m}_{\mathrm{in}} - \dot{m}_{\mathrm{out}}) - k\frac{P}{V}\dot{V} \tag{4}$$

While the discharging process is regarded as isothermal, i.e., $T =$ constant,

$$\dot{P} = \frac{RT}{V}(\dot{m}_{\mathrm{in}} - \dot{m}_{\mathrm{out}}) - \frac{P}{V}\dot{V}. \tag{5}$$

Note that Eqs. (3) and (4) is just different from the specific heat ratio term k. Thus according to both equations, the common process between charging and discharging processes can be expressed as:

$$\dot{P} = \frac{RT}{V}(\alpha_{\mathrm{in}}\dot{m}_{\mathrm{in}} - \alpha_{\mathrm{out}}\dot{m}_{\mathrm{out}}) - \alpha\frac{P}{V}\dot{V}, \tag{6}$$

with α_{in}, α_{out} and α taking values between 1 and k, depending on the actual heat transfer during the process. Here, $\alpha_{in} = 1$ and $\alpha_{out} = k = 1.4$, namely we consider charging process is absolute adiabatic while discharging is isothermal, and $\alpha = 1.2$ [12].

3.2. The mathematic model of on–off valve

In the pneumatic system, the valve is the command component and there are many different types of valves by the geometry of the orifice, the flow regulating and so on. Here our model is just restricted to the on–off spool valve. We choose the MHP2-MS1H high-speed on–off valve of Festo Inc. with up to 500 Hz on–off frequency, as Fig. 4 shown. It is convenient to realize the position or force servo control through the variable PWM signals.

The on–off valve character is always described by the on and off time character, as it has only on and off two states. Assuming that the spool displacement changes linearly during the on and off process, thus the on-time t_{on} is composed of armature picking up time t_1 and spool responding time t_2, namely $t_{on} = t_1 + t_2$; instead the off-time t_{off} is composed of armature taking down time t_3 and spool releasing time t_4, namely $t_{off} = t_3 + t_4$. So the on–off characteristic of the valve is:

$$X_i = \begin{cases} 0 \\ \quad t \in [(i-t)T_c,\ (i-1)T_c + t_1] \\ \frac{X_m}{t_2}[t - (i-1)T_c - t_1] \\ \quad t \in [(i-t)T_c + t_1, (i-1)T_c + t_1 + t_2] \\ X_m \\ \quad t \in [(i-t)T_c + t_1 + t_2, (i-1)T_c + t_p + t_3] \\ -\frac{X_m}{t_4}[t - (i-1)T_c - t_p - t_3 - t_4] \\ \quad t \in [(i-t)T_c + t_p + t_3, (i-1)T_c + t_p + t_3 + t_4] \\ 0 \\ \quad t \in [(i-t)T_c + t_p + t_3 + t_4, iT_c], \end{cases} \tag{7}$$

where, X_i – the spool displacement; X_m – the spool maximum displacement; T_c – period of PWM signal; t_p – the width of the high-voltage in one PWM period. Fig. 5 depicts the on–off characteristic of the valve intuitionally and t_{on} and t_{off} in one PWM period.

Fig. 4. The MHP2-MS1H high-speed on–off valve of Festo Inc.

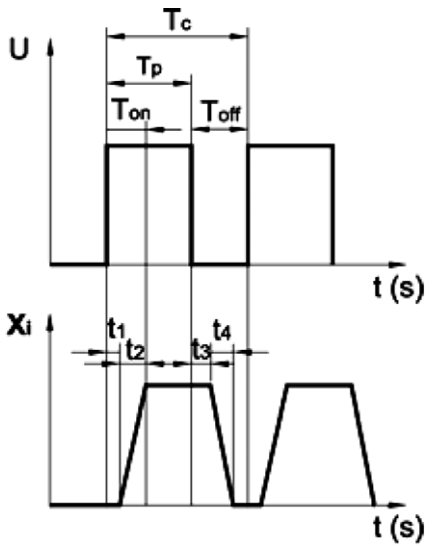

Fig. 5. The on–off characteristic of the on–off valve.

The possible flow patterns in the valve can be categorized depending on the ratio of upstream pressure to downstream pressure [11]. The standard equation for the mass flow through an orifice of area A_v is:

$$\dot{m}_v = \begin{cases} C_f A_v C_1 \frac{P_u}{\sqrt{T}} & \text{if} \quad \frac{P_d}{P_u} \leqslant P_{cr} \\ C_f A_v C_2 \frac{P_u}{\sqrt{T}} \left(\frac{P_d}{P_u}\right)^{1/k} \sqrt{1 - \left(\frac{P_d}{P_u}\right)^{(k-1)/k}} & \text{if} \quad \frac{P_d}{P_u} > P_{cr}, \end{cases} \tag{8}$$

where, $\dot{m}_v$ is the flow through the valve orifice, C_f the coefficient of flow, P_u the upstream pressure, P_d the downstream pressure, and

$$C_1 = \sqrt{\frac{k}{R}\left(\frac{2}{k+1}\right)^{\frac{k+1}{k-1}}}, \quad C_2 = \sqrt{\frac{k}{R}\left(\frac{2}{k-1}\right)},$$
$$P_{cr} = \left(\frac{2}{k+1}\right)^{\frac{k}{k-1}}. \tag{9}$$

According to the load, the valve spool dynamic expression is:

$$M\ddot{X} + B\dot{X} + KX + F_r + F_l = P_1 A_1 - P_2 A_2 - P_a(A_1 - A_2), \tag{10}$$

in which M is the mass of the load, B is the damp coefficient, K is spring constant, F_r is the friction force, F_l is the load force and P_a is the pressure of atmosphere. P_1, P_2 and A_1, A_2 are shown in Fig. 3.

3.3. Connecting tube model

The Arm-Exoskeleton, ZJUESA is designed as a wearable master arm for the robot manipulator teleoperation with the force-feedback. Due to design and weight considerations, the on–off valves are positioned at relatively large distance from the pneumatic cylinders. Thus, the effects of

time delay and attenuation of pressure input due to the connecting tubes become significant. Thus in our force-feedback system model, we also pay attention to the effect of the connecting tubes.

The two basic equations governing the flow in a circular pneumatic line are derived as,

$$\frac{\partial P}{\partial s} = -R_t u - \rho \frac{\partial u}{\partial t}, \tag{11}$$

$$\frac{\partial u}{\partial s} = -\frac{1}{\rho c^2}\frac{\partial P}{\partial t}, \tag{12}$$

where, P is the pressure along the tube, u is the flow velocity in the tube, c is the sound velocity, s is the tube axis coordinate, R_t is the resistance between the air flow and the tube. It can be calculated as:

$$R_t = \begin{cases} \frac{32\mu}{D^2} & \text{if laminar flow,} \\ \frac{0.158\mu}{D^2} Re^{3/4} & \text{if turbulent flow,} \end{cases} \tag{13}$$

where, μ is the dynamic viscosity of the air, Re is Reynolds number, D is the inner diameter of the tube.

Part differentiating Eq. (11) with t and Eq. (12) with s respectively, the equation for the mass flow can be rewritten as,

$$\frac{\partial^2 \dot{m}_t}{\partial t^2} - c^2 \frac{\partial^2 \dot{m}_t}{\partial s^2} + \frac{R_t \partial \dot{m}_t}{\rho \partial t} = 0. \tag{14}$$

It is the general wave equation. With the certain initial and boundary condition, we can solve it and get the following solution:

$$\dot{m}_t(L_t, t) = \begin{cases} 0 & \text{if} \quad t < L_t/c, \\ e^{-\frac{R_t R T L_t}{2P c}} h\left(t - \frac{L_t}{c}\right) & \text{if } t > L_t/c, \end{cases} \tag{15}$$

where, L_t is the length of the tube and $h(t)$ is the flow input at the tube inlet.

Note that the tubes connecting the valve with the actuator have two effects on the system response. Firstly, the pressure drop along the tube will induce a decrease in the steady state airflow through the valve. Secondly, the flow profile at the outlet will be delayed with respect to the one at the inlet by the time increment necessary for the acoustic wave to travel the entire length of the tube [2]. Thus in practice a feedback scale is introduced to compensate the dropping pressure, and the disposal of the system should be optimized to shorten the line length or a prediction algorithm should be adopted in the future work.

4. The hybrid fuzzy control algorithm and controller design

In the above sections, we model the influence of three types of pneumatic components, including cylinder, on–off valve and connecting tube. There are a great number of control algorithms that can be found to control the above system. In this part, we give out the control algorithm and controller design for the ZJUESA pneumatic force-feedback system.

The pneumatic system is usually not a well linear control system, because of the air compressibility and its effect on the flow line. Also the highly nonlinear flow brings troubles into the control. As a result, the conventional controllers are often developed via simple models of the plant behavior that satisfy the necessary assumptions, and via the specially tuning of relatively simple linear or nonlinear controllers. For pressure or force control in such a nonlinear system, especially in which the chamber pressure vibrates rapidly, even in one PWM on–off period, the conventional control method can hardly have a good performance.

The introduction of the hybrid control method gives out a solution to this problem. However, as the ANFMRC mentioned in the Ref. [13], the design of the hybrid controller is always complicated and only available to the proportion or servo valve system. In our system, we figured out a hybrid fuzzy control method for the high-speed on–off valves, which is much simpler and can be realized by MCUs in the contributed architecture.

Fig. 6 shows the structure of the proposed hybrid controller. Bang-bang control is applied when the actual output is far away from reference value. In this mode, fast tracking of the output is required. The fuzzy controller is activated when the output is near the set point, which needs accurate control. The fuzzy controller provides a formal methodology for representing, manipulating, and implementing a human's heuristic knowledge about how to control a system [15]. It can be regarded as an artificial decision maker that operates in a closed-loop system in real time. The system can get the control information either from a human decision maker who performs the control task or by self-study. The hybrid controller switch condition can be described as:

$$\text{controller} = \begin{cases} \text{bang-bang controller} & \text{if error} \geqslant |E|, \\ \text{fuzzy controller} & \text{if error} < |E|. \end{cases} \tag{16}$$

Fig. 7 explains the scheme of the fuzzy control mode in the hybrid fuzzy controller for the pneumatic force-feedback system. We use pressure error $e(t) = P_r(t) - P_1(t)$ and change in error $\dot{e}(t) = \frac{d}{dt}e(t)$ as the input variables on which to make decisions. As there are rapid vibrations of the pressure in a small interval, the change in error of the pressure is often not consistent to the changing tendency of the average pressure for a long period. So we introduce the gains on the proportional and derivative terms to weak its irregular influence. The gain on proportional term is taken as 9 and 1 for the derivative term. On the other hand, the width of the high-voltage in one PWM period t_p is denoted as the output u of the controller, which drives the valve to switch. During the course of high-voltage, the cylinder chamber is link to the high-pressure, and vice versa. Whether the cylinder chamber connects to the high-pressure or atmosphere, we could determine the flow by

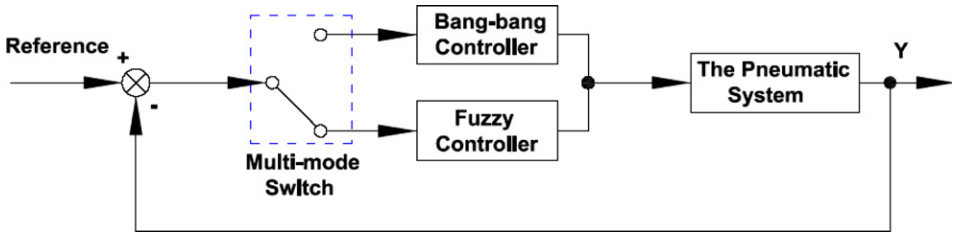

Fig. 6. The concept of the hybrid controller.

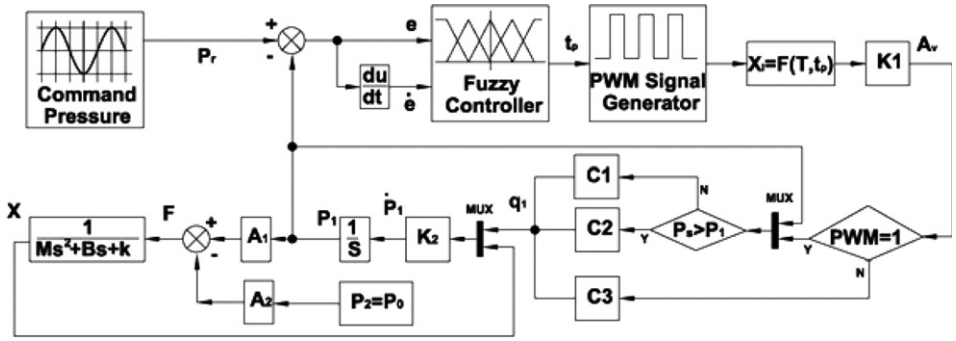

Fig. 7. The scheme of the fuzzy control mode of the hybrid controller in the pneumatic force-feedback system.

Eqs. (8) and (9) with relative coefficient C_1, C_2 and C_3 due to the pressure ratio. With the second-order model of load and rod, the block of force-feedback control can be deduced.

Here we use the following fuzzy model to represent a complex two-input single-output system that includes both approximation inference rules and local analytic models.

$$\mathbf{R}^{\mathbf{L}}\text{: if } e(t) = A_i \quad \text{and} \quad \dot{e}(t) = B_j, \quad \text{then } u = U_{ij}, \tag{17}$$

where $\mathbf{R}^{\mathbf{L}}$ denotes the lth approximation inference rule. A_i and B_j are the values of the two inputs, error $e(t)$ and $\dot{e}(t)$ change in error, and U_{ij} is the output variable of the system. In fuzzy control the relation between the output and the inputs can be generally expressed with a nonlinear function. It is can be intuitively depicted by Fig. 8. In this figure each bounded monotonic curve represents $u(t)$ for a different value $\dot{e}(t)$. They can be expressed by Eq. (18) [22].

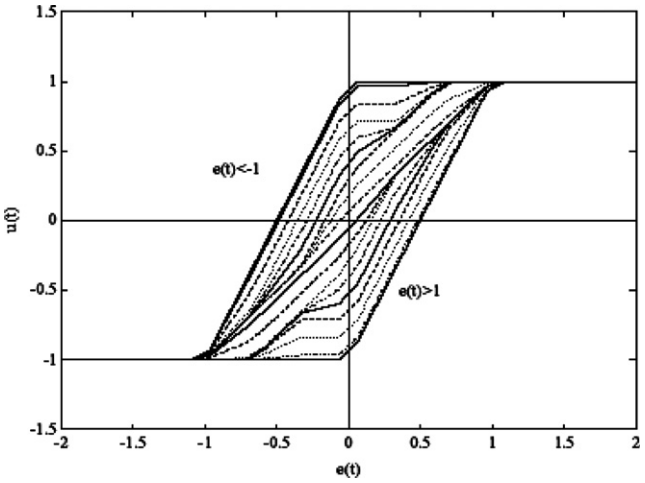

Fig. 8. Fuzzy controller characteristic curve [23].

$$U(-e, \dot{e}) = \frac{k_i(\mathrm{e}^{-a_i E} - 1)}{\mathrm{e}^{-a_i E} + 1} + K_i \cdot E_{\mathrm{c}}, \tag{18}$$

where k_i, a_i, and K_i are the coefficients. k_i determines the altitude of the curve; K_i expresses whether the curve pass through the original point or not; a depicts the shape of the curve. E and E_{c} are the fuzzy sets of the two input $e(t)$ and $\dot{e}(t)$ respectively.

In the work of Barth et al. state-space averaging can be utilized to convert the switching model given in Eqs. (1)–(6), (8)–(15) to a continuous average model. The average model is formed in the s-domain as:

$$\hat{G}(s) = \frac{F(s)}{\hat{U}(s)} = \frac{K\mathrm{e}^{-T_{\mathrm{D}}s}P(s)}{M\tau s^3 + Ms^2} \tag{19}$$

where, τ is the time constant, which is a typically nonlinear function of the upstream and downstream and so on. T_{D} is the time delay exhibited between the control command and the pressure dynamic.

The average model given by Eq. (19) assumes that the input $\hat{u}(t)$ can vary continuously in time, which is not the case. Specifically, once a given duty cycle is commanded, the control command cannot be changed until the next PWM period or next sampling period. The control command is therefore subjected to a sample-and-hold operation. Given the standard frequency domain approximation of a sample-and-hold, the transfer function of the average model from the continuous control command $u(t)$ to the motion of the output $f(t)$ can be given as:

$$G(s) = \frac{F(s)}{U(s)} = \frac{1 - e^{-Ts}}{Ts} \cdot \frac{Ke^{-T_D s}P(s)}{M\tau s^3 + Ms^2}. \quad (20)$$

Also such SISO system can be reformed with space-state method as:

$$\begin{cases} \dot{X} = AX + BU, \\ Y = CX, \end{cases} \quad (21)$$

where A is $n \times n$ state transition matrix, B, X is the $n \times 1$ state vector, C is the $1 \times n$ state vector, Y and U are the input and output respectively. By replacing the input U with Eq. (18) and Eq. (21) can be rewritten in the following form:

$$\begin{cases} \dot{X} = AX + B\left[k\frac{e^{aE}-1}{e^{aE}+1} \cdot K\dot{E}\right], \\ Y = CX, \end{cases} \quad (22)$$

where $k \in k_i$ and $K \in K_i$ in Eq. (18) [22].

In general, when the input is 0, $E = -Y$. As a result, Eq. (22) can be explained as following:

$$\dot{X} = A'X + B'\frac{e^{-acX} - 1}{e^{-acX} + 1} = f(x), \quad (23)$$

where $A' = [I + KBC]^{-1}A; B' = k[I + KBC]^{-1}B$.

In the Lyapunov's second or direct method, let $x_e = 0$ be an equilibrium for Eq. (23). Let Lyapunov function V: be a continuously differentiable function such that $V(0) = 0$ and $V(x) > 0$, and $\dot{V}(x) < 0$. Then $x_e = 0$ is stable. For the

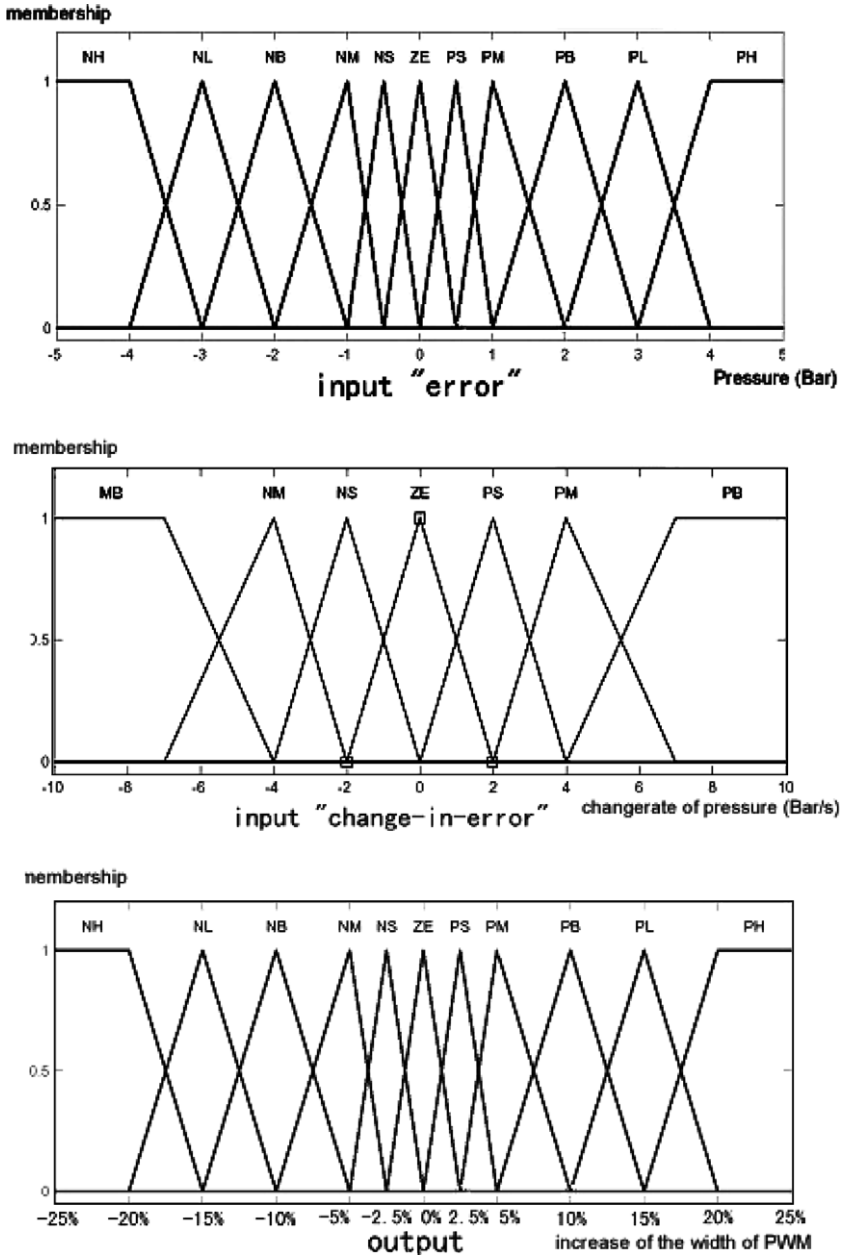

Fig. 9. The membership functions for the fuzzy controller.

Table 1
Rule table for the fuzzy controller

"Output" u		"Error" e										
		PH	PL	PB	PM	PS	ZE	NS	NM	NB	NL	NH
"Change-in-error" $\dot{e}$	PB	PH	PH	PL	PL	PB	PM	PS	NS	NM	NM	NB
	PM	PH	PL	PL	PB	PM	PS	NS	NS	NS	NM	NB
	PS	PL	PL	PB	PB	PM	ZE	ZE	NS	NM	NB	NB
	ZE	PL	PB	PB	PM	PS	ZE	NS	NM	NB	NB	NL
	NS	PB	PB	PM	PS	ZE	ZE	NM	NB	NB	NL	NL
	NM	PB	PM	PS	PS	PS	NS	NM	NB	NL	NL	NH
	NB	PB	PM	PM	PS	NS	NM	NB	NL	NL	NH	NH

PH – positive huge; PL – positive large; PB – positive big; PM – positive middle; PS – positive small; ZE – zero; NH – negative huge; NL – negative large; NB – negative big; NM – negative middle; NS – negative small.

system described by Eq. (23), the Krasovskii method is employed to construct the Lyapunov function V.

$$V(x) = f^T(x)f(x). \tag{24}$$

According to the stable condition of the system, $\dot{V}(x) = \frac{\partial f(x)}{\partial t} + \frac{\partial f^T(x)}{\partial t} < 0$, the domain of coefficients k and K can be obtained. This gives the rule for fuzzy controller designing and ensures the stability of the system.

Fig. 9 depicts the membership functions of the input "error", "change-in-error" and the output "u". There are 11 intervals for the pressure error and 7 intervals for the derivative term. Also 11 classes are allocated to the output. Membership function in the fuzzy layer is commonly a symmetric function, such as bell shape function, triangle function, or trapezoidal function. In this paper all the membership functions are dictated by the skewed triangle membership function for its simplicity, but the membership functions are narrower near zero. This serves to decrease the gain of the controller near the set point so we can obtain a better steady-state control and yet avoid excessive overshoot spacing of the output membership function. The rule base array that we use for the controller is shown in Table 1.

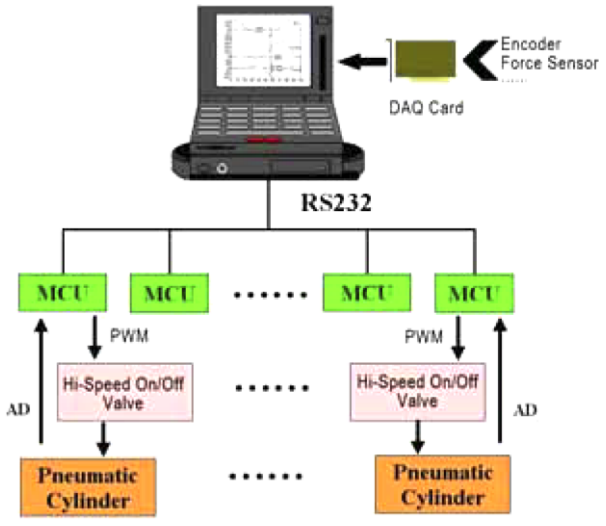

Fig. 10. The distributed pneumatic control architecture of the pneumatic force-feedback system.

In practice, we design the hybrid fuzzy control system in the form of distributed control architecture, as Fig. 10 shown. Each Mega8 MCU of ATMEL Inc. works as a hybrid fuzzy controller for each cylinder respectively, and forms a pressure closed-loop control. The controller samples the pressure in chamber with 2000 Hz sampling rate by the AD converter affiliated to the MCU. Since the sampling values tend to jump up and down with the pressure, a median filter is used to average the sampling pressure value amid the 4 PWM periods, which is as the feedback pressure in the closed-loop.

5. Implementation

The implementation can be divided into two parts, hardware and software. As seen in Fig. 11, the system includes the soft signal generator and data acquisition, Mega8 MCU experiment board, on–off valves, sensors of displacement and pressure, and the oscilloscope. We chose the cylinder DSNU-10-40-P withΦ10 mm and 40 mm length, produced by FESTO Inc., and fixed the piston of the cylinder at the middle of the stroke. The system obtains the reference signal and sends the experimental data through the RS232 and implements the force control by means of the hybrid fuzzy controller on the MCU experiment board.

The soft signal generator and data acquisition are two main parts of the software. Both are designed in the LabVIEW, with which users may take advantage of its powerful graphical programming capability. Compared to other conventional programming environment, the most obvious difference is that LabVIEW is a graphical compiler that uses icons instead of lines of text. Additionally LabVIEW has a large set of built-in mathematical functions and graphical data visualization and data input objects typically found in data acquisition and analysis applications. Here the software generates the reference pressure and force and shows the experimental data on the screen. The RS232 bridges the software and hardware.

6. Simulations and experiments

A simulation of the pneumatic system model and hybrid fuzzy controller was implemented in MATLAB. Simulated

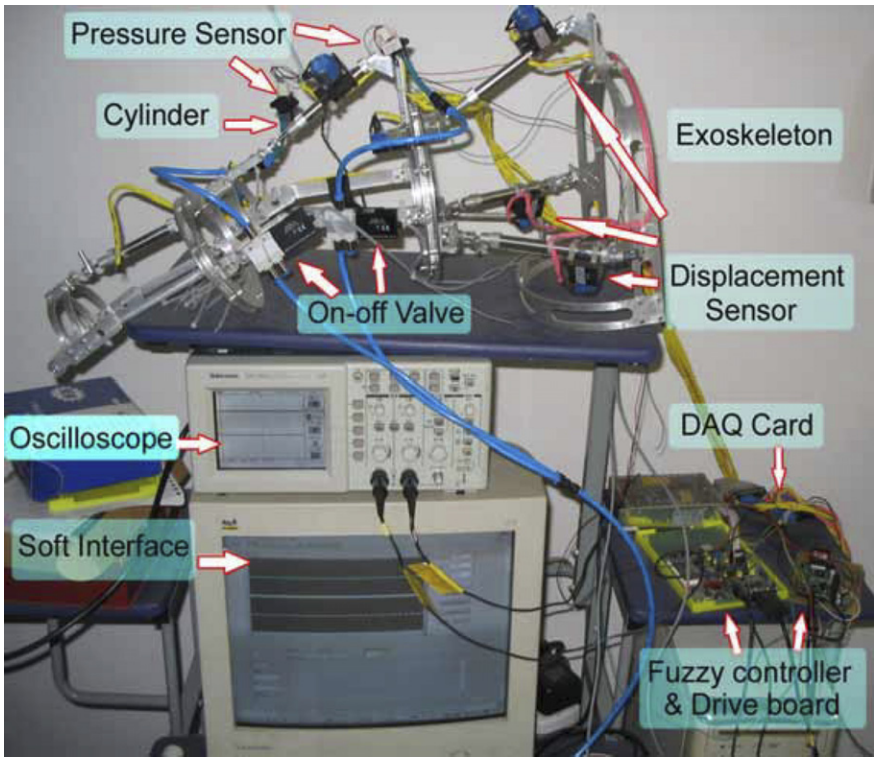

Fig. 11. The experiment set-up.

results of how the pressure in the cylinder chamber behaves under certain conditions were produced. In addition, three sets of experiments were conducted in this section to validate the mathematical model and fuzzy control method. In the experiments we measured the pressures in both cylinder chambers by the MPX 5500 integrated silicon pressure sensors of Freescale Inc., which are state-of-the-art monolithic silicon pressure sensors on-chip signal conditioned, temperature compensated and calibrated [24]. The signals measured by these devices are then transferred to the forces provided by the actuator. Also the errors between these outputs and references and its change are considered as the inputs of the controller to make the closed-loop controller.

Figs. 12 and 13 give both the numerical and experimental results of the chamber pressure and force outputs with different amplitude step input signals. After smoothed, both the pressure and the force output curves track the reference and numerical curves very well with very good amplitude match and less than 0.01 s misalignment in the time profiles.

The plots in Figs. 14 and 15 give the results of the chamber pressure and actuator force outputs by following a ramped input. Due to the compressibility and the nonlinear character of the air media, there are some waves along the output curve. As a whole, the output curves perform a good control character to track the input signal. The errors of the pressure and force of the slope input are shown in Figs. 16 and 17, respectively. Note that the errors are almost negative and positive errors are always very small,

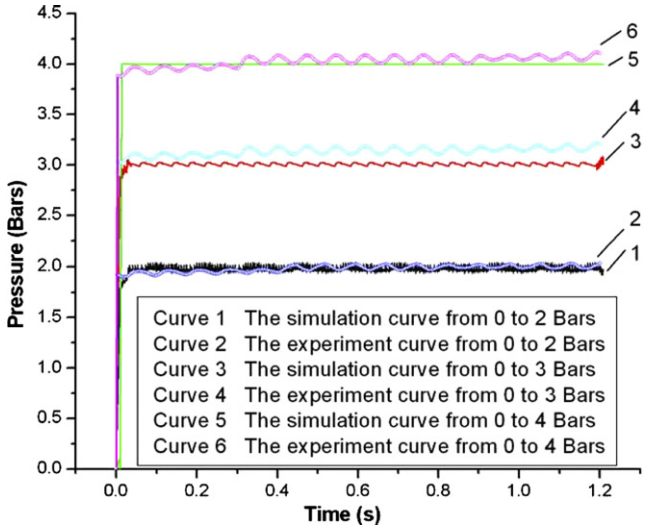

Fig. 12. The simulation numerical and experimental results corresponding to different pressure step signals.

which ensures the safety of the force-feedback in a certain extent.

In the other sets of experiments, we use series of sinusoidal commands with different frequencies to measure the dynamitic nature of the system. As Fig. 18 shows, the frequencies of sinusoidal signals are 5 Hz and 2.5 Hz. Although there is a little error between the reference curve and the experiment curve in the rising part of the signals, the system has a good performance.

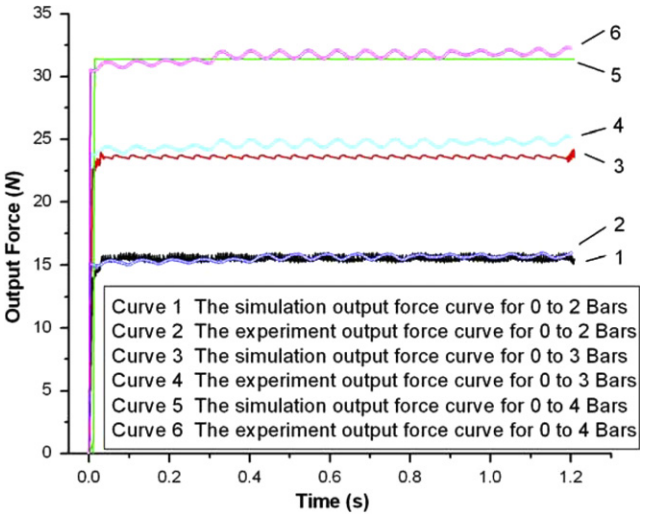

Fig. 13. The simulation and experiment results of output force with different amplitude step signals.

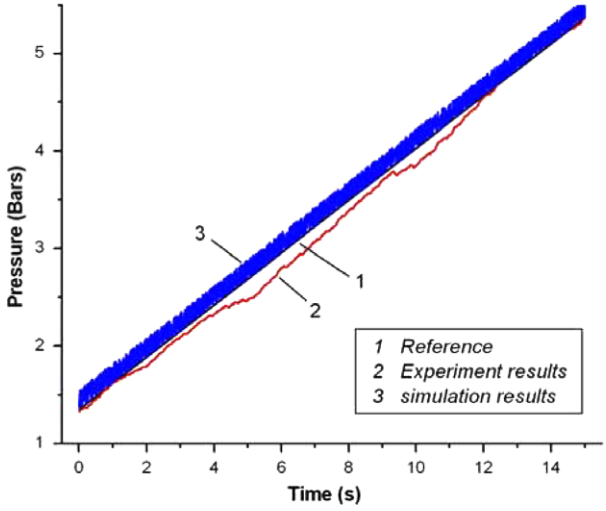

Fig. 14. The experimental result of pressure for a ramped input.

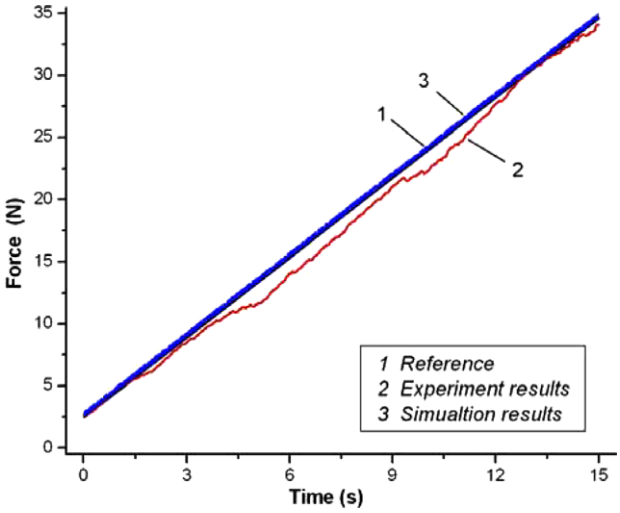

Fig. 15. The experimental result of force for a ramped input.

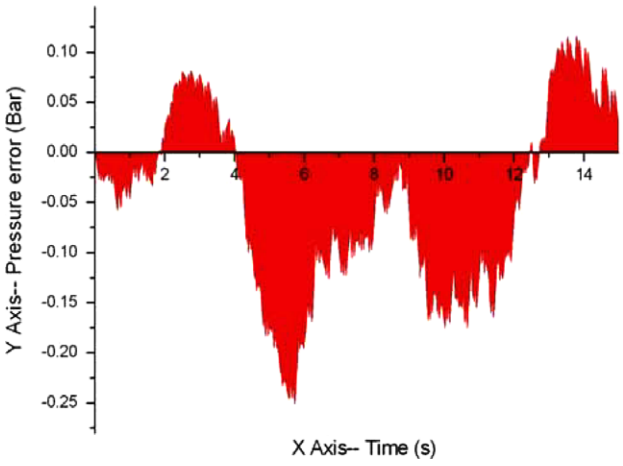

Fig. 16. The pressure errors of the ramped input.

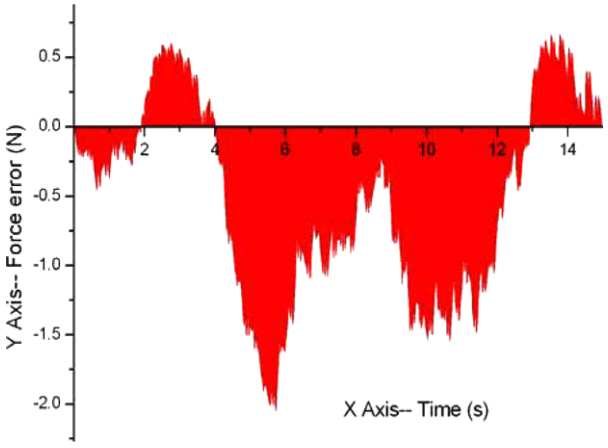

Fig. 17. The force errors of the slope input.

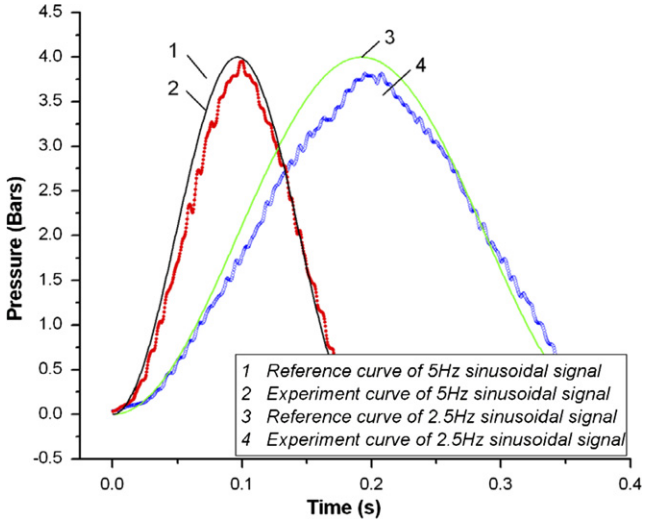

Fig. 18. Experimental results for 5 Hz and 2.5 Hz sinusoidal pressure commands.

There are some remarks. Despite the fact that there are quickly vibrations of the pressure in the chamber amid a 1 ms or even smaller interval, the output is so smooth as the lag of operator's feeling and the high-frequency (above 30 Hz) information carries little energy. While at frequencies lower than 2.5 Hz, force is sensed through the operator's joint, muscle and tendon receptors, and the operator is able to respond to, and stabilize, low-amplitude disturbances at these frequencies [19]. We use the Fourier transform to remove reflected force signals above 20 Hz for simulating operator's feeling and get the smoothed curve in each plot.

7. Conclusions

In this article we describe a new application of the pneumatic system and its hybrid fuzzy controller. The pneumatic actuators are used as the force-feedback system for the master type exoskeleton, ZJUESA, with the control by the on/off valve for improving the master/slave manipulating characteristics. In the controller design the mathematical models of the pneumatic system are given. The models include pneumatic cylinder and high-speed on–off valve by considering the compressibility and nonlinearity of the air, which are simple and effective. In the meanwhile, we also take the effects of time delay and attenuation due to the connecting tubes into account with the purpose of force fidelity and real time control. Based on the models, the hybrid fuzzy control method is used and its controller is designed with the Mega8 MCU. The results are obtained by both simulations in MATLAB and experimental researches. In the experiments, step, slope and sinusoidal commands are taken and the system shows a good performance, and a good agreement is found between the numerical and experimental curves as well. In the future work, the dynamic friction of the piston in the cylinder and viscous friction of valve will be added into the models, and the improved models and control method will be used to have a better manipulation effect.

Acknowledgements

The support provided by National Natural Science Foundation of China (No. 50305035) is greatly appreciated. The authors gratefully acknowledge our lab-mate Mr. Hu Biao for sharing his knowledge of the pneumatic experiment and programing. Authors' thanks must go to Festo Co. China for its experiment equipment donation.

References

[1] Ephanov A, Stoianovici D. Effect of a pneumatically driven haptic interface on the perceptional capabilities of human operators. Presence 1998;7(3):290–307.

[2] Richer E, Hurmuzlu Y. A high performance pneumatic force actuator system. ASME J Dyn Syst Meas Control 2000;122(3):416–425.

[3] Goertz R. Manipulator systems development at ANL. In: Proc of 12th Conf Remote Syst Technol 1964, p. 12.

[4] Schiele A. Development of a human arm exoskeleton for space robotics telepresence: from biomechanics to mechanism design. ESA Final Report, EWP–2161, November 2001.

[5] Jeong YK, et al. A wearable robotic arm with high force-reflection capability. In: Proc of the IEEE Int Workshop on Robot and Human Interactive Communication 2000, p. 411–6.

[6] Pfeiffer C, Mavroidis C, et al. Electrorheological fluid based force feedback device. In: Proc of the SPIE Telemanipulator and Telepresence Technologies VI Conference 1999; 3840, p. 88–99.

[7] Kim YS, et al. A new exoskeleton-type masterarm with force reflection based on the torque sensor beam. In: Proc of the IEEE Int Conf on Robotics and Automation 2001, p. 2628–33.

[8] Kim YS et al. A force reflected exoskeleton-type masterarm for human–robot interaction. IEEE Trans Syst Man Cybernet Part A: Syst Humans 2005;35(2):198–212.

[9] Bobrow JE, Jabbari F. Adaptive pneumatic force actuation and position control. J Dyn Syst Meas Control 1991;113:267–72.

[10] Ben-Dov D, Salcudean SE. A force-controlled pneumatic actuator. IEEE Trans Robot Automat 1995;11(6):906–11.

[11] Tressler JM, Clement T, Kazerooni H, Lim M. Dynamic behavior of pneumatic systems for lower extremity extenders. In: Proc of the IEEE Int Conf Robotics Automation 2002, p. 2348–53.

[12] Al-Ibrahim AM, Otis DR. Transient air temperature and pressure measurements during the charging and discharging processes of an actuating pneumatic cylinder. In: Proc of the 45th National Conf on Fluid Power, 1992.

[13] Kaitwanidvilai S, Parnichkun M. Force control in a pneumatic system using hybrid adaptive neuro-fuzzy model reference control. Mechatroincs 2005;15:23–41.

[14] Yang CJ, Niu B, Zhang JF, Chen Y. Different structure based control system of the PUMA manipulator with an arm exoskeleton. In: Proc of the IEEE Conf on Robotics, Automation and Mechatronics, Singapore 2004, p. 572–7.

[15] Passino KM, Yurkovich S. Fuzzy control. Addison-Wesley Longman, Inc.; 1998.

[16] Ahn K, Yokota S. Intelligent switching control of pneumatic actuator using on/off solenoid valves. Mechatroincs 2005;15:683–702.

[17] Shih MC, Ma MA. Position control of a pneumatic cylinder using fuzzy PWM control method. Mechatronics 1998;8:241–53.

[18] Messina A, Giannoccaro NI, Gentile A. Experimenting and modelling the dynamics of pneumatic actuators controlled by the pulse width modulation (PWM) technique. Mechatroincs 2005;15:859–81.

[19] Thompson RL. Integration of visual and haptic feedback for teleoperation. PhD thesis, Department of Engineering Science University of Oxford, 2001.

[20] Barth EJ, Zhang JL, Goldfarb M. Control design for relative stability in a PWM-controlled pneumatic system. J Dyn Syst Meas Control 2003;125:504–8.

[21] Yin YB, Araki K. Modelling and analysis of an asymmetric valve-controlled single-acting cylinder of a pneumatic force control system. In: Proc of SICE '98, p. 1099–104.

[22] Xu WL, Wu RH. Lyapunov's indirect method for stability analysis of fuzzy control system. J Hunan Univ (Natural Sci) 2004;31(3):86–9 [in Chinese].

[23] Jenkins D, Passino KM. An introduction to nonlinear analysis of fuzzy control systems. J Intell Fuzzy Syst 1999;7(1):75–103.

[24] Available from: http://www.freescale.com/webapp/sps/site/taxonomy.jsp?nodeId=01126990368716.